NASA CR-165580

R82AEB189

National Aeronautics and
Space Administration

CF6 JET ENGINE DIAGNOSTICS PROGRAM

HIGH PRESSURE COMPRESSOR CLEARANCE INVESTIGATION

by

M.A. Radomski

GENERAL ELECTRIC COMPANY

JANUARY 1982

Prepared For

National Aeronautics and Space Administration

NASA Lewis Research Center

CONTRACT NAS3-20631

1. Report No. NASA CR-165580	2. Government Accession No.	3. Recipient's Catalog No.
4. Title and Subtitle CF6 JET ENGINE DIAGNOSTICS PROGRAM- HIGH PRESSURE COMPRESSOR CLEARANCE INVESTIGATION		5. Report Date January 1982 6. Performing Organization Code
7. Author(s) M. A. Radomski		8. Performing Organization Report No. R82AEB189 10. Work Unit No.
9. Performing Organization Name and Address General Electric Company Aircraft Engine Group Cincinnati, Ohio 45215		11. Contract or Grant No. NAS3-20631 13. Type of Report and Period Covered Contractual Report
12. Sponsoring Agency Name and Address National Aeronautics and Space Administration Washington, D. C. 20543		14. Sponsoring Agency Code

15. Supplementary Notes

Project Manager, J. McAulay
NASA Lewis Research Center
Cleveland, Ohio

Project Engineer, R.P. Dengler

16. Abstract

The effects of high pressure compressor clearance changes on engine performance were experimentally determined on a CF6 core engine. The results indicate that a one percent reduction in normalized average clearance, expressed as a fraction of airfoil length, improves compressor efficiency by one percent.

Compressor cleanances can be reduced by the application of rotor bore cooling, insulation of the stator casing and use of a low coefficient of expansion material in the aft stages. This improvement amounts to a reduction of normalized average clearance of 0.78 percent, relative to the CF6-50 compressor, which is equivalent to an improvement in compressor efficiency of 0.78 percent.

17. Key Words (Suggested by Author(s))	18. Distribution Statement
Jet Engine Compressor Clearance Turbofan Engine Performance Deterioration	Unclassified unlimited

19. Security Classif. (of this report)	20. Security Classif. (of this page)	21. No. of Pages	22. Price*
Unclassified	Unclassified	42	

* For sale by the National Technical Information Service, Springfield, Virginia 22161

FOREWORD

The work was performed by the Evendale Product Engineering Operation of General Electric's Aircraft Engine Group, Aircraft Engine Engineering Division, Evendale, Ohio. The program was conducted for the National Aeronautics and Space Administration, Lewis Research Center, Cleveland, Ohio, under Subtask 5.1 of the CF6 Jet Engine Diagnostics Program, Contract Number NAS3-20631. The CF6 Jet Engine Diagnostics Program is part of the Engine Component Improvement (ECI) Project, which is part of the NASA Aircraft Energy Efficiency (ACEE) Program. The NASA Project Engineer for this program was R. P. Dengler. The program was initiated in January 1980 and completed in May 1981. The General Electric Program Manager was W. A. Fasching. Technical work, including the preparation of the report, was done by M. A. Radomski, with the help of M. Miller, G. Oxenham, W. Multner, D. Chan and D. Leachman. D. Simons and S. Hong supervised engine build-up and test.

TABLE OF CONTENTS

LIST OF ILLUSTRATIONS

LIST OF ILLUSTRATIONS (Concluded)

1.0 SUMMARY

In the CF6 Jet Engine Diagnostic Program the causes of performance degradation were determined for each component of revenue service engines. It was found that a significant contribution to performance degradation was caused by increased airfoil tip radial clearances in the high pressure compressor.

The objective of this investigation was to conduct a systematic test program to evalute the effects of high pressure compressor clearance changes on engine performance and to examine potential clearance improvements for both steady state and transient operation. The potential methods of clearance improvements included rotor bore cooling, insulating the aft stages of the stator casing, and reducing the thermal coefficient of expansion of the stator casing material in these stages.

Core engine tests were conducted with an instrumented high pressure compressor. The special instrumentation included pressure and temperature rakes at compressor inlet and discharge, pressure and temperature probes in the cooling airflow stream, stator casing and rotor structure thermocouples and blade tip clearanceometers.

Both steady-state power calibration and transient engine test runs were made. The power calibrations were made with several different compressor clearances which were produced by varying the rotor bore cooling airflow. In the transient tests, the cooling airflow was maintained at a constant fraction of the engine airflow and was used as a means of clearance improvement.

The results of the steady-state power calibration indicate that, if clearance change is expressed as a fraction of the airfoil length, a one percent clearance reduction improves compressor efficiency by one percent. The results of the transient tests show that significant improvements in clearances can be obtained by the use of rotor bore cooling, insulation of the stator casing and use of low coefficient of expansion material for the stator casing in the aft stages of the compressor. Calculations indicate that clearances in the rear stages can be reduced by 1.0 mm (0.040 in) relative to the current CF6-50 compressor. This would produce a normalized average clearance change of 0.78 percent which is equivalent to an improvement in compressor efficiency of 0.78 percent.

The clearance improvement features tested in this program are being utilized in the new CF6-80 compressor.

2.0 INTRODUCTION

A program was initiated for the CF6 family of turbofan engines to identify and quantify the causes of performance deterioration which increase fuel consumption. The recent energy demand has outpaced domestic fuel supplies, creating an increased United States dependence on foreign oil. This increased dependence was accentuated by the OPEC embargo in the winter of 1973-1974 which triggered a rapid rise in the price of fuel. This price rise, along with the potential for further increases, brought about a set of changing economic circumstances with regard to the use of energy. These events were felt in all sectors of the transportation industry. As a result, the Government, with the support of the aviation industry, initiated programs aimed at both the supply and demand aspects of the problem. The supply aspect is being investigated by determining the fuel availability from new sources such as coal and oil shale, with concurrent programs in progress to develop engine combustors and fuel systems to accept these broader based fuels.

Reduced fuel consumption is the approach being employed to deal with the demand aspect of the problem. Accordingly, NASA is sponsoring the Aircraft Energy Efficiency (ACEE) program which is directed toward reducing fuel consumption for commercial air transports. The long-range effort to reduce fuel consumption is expected to evolve new technology which will permit development of a more energy efficient turbofan, or an improved propulsion cycle such as that for turboprops. Studies have indicated that large reductions in fuel usage are possible (e.g., 15 to 40 percent); from this approach, however, a significant impact in fuel usage is considered to be 15 or more years away. In the near term, the only practical propulsion approach is to improve the fuel efficiency of current engines since these engines will continue to be the significant fuel users for the next 15 to 20 years.

The Engine Component Improvement (ECI) program is the element of the ACEE program directed at improving the fuel efficiency of current engines. The ECI program consists of two parts: (1) Performance Improvement and (2) Engine Diagnostics. The Performance Improvement program is directed at developing engine performance improvement and retention concepts for new production and retrofit engines. The Engine Diagnostics effort is to provide deterioration information for the high bypass ratio turbofan engines utilized on wide-body aircraft.

As part of the Engine Diagnostics effort, NASA-Lewis initiated a program with the General Electric Company to conduct high pressure compressor clearance evaluations.

Compressor performance is known to be significantly influenced by variations in compressor airfoil tip clearances. The new engine clearances are dictated primarily by the differential thermal and elastic growths of the compressor rotor and stator structures that occur during transient and steady-state operating conditions. In current designs, such as the CF6-50 compressor, the transient thermal response of the rotor structure is much slower than that of the stator

structure. This characteristic results in larger steady-state running clearances than are desirable for good performance. Smaller clearances can, therefore, be achieved by improving the match of the stator and rotor structures thermal responses i.e. by slowing down the stator and speeding up the rotor thermal responses.

Field experience has shown that for the typical performance deterioration of a CF6-50 engine after 4000 hours of revenue service, an increase in SFC of about 0.7% is due to high pressure compressor performance loss (Ref. 1). This was based to a large extent on the examination of service hardware and calculating the performance effect rather than component performance measurements obtained from engine tests. Verification of this contribution was, therefore, necessary using controlled engine tests with measured clearance variations.

The scope of this program was to establish, more precisely than heretofore, the influence of compressor clearance variations on engine performance and to evaluate potential improvements that could be made in the steady-state and transient clearances. To determine the influence of compressor clearance variations on engine performance, instrumented core engine tests were conducted in which compressor airfoil tip clearances were varied by varying the compressor rotor bore cooling airflow at steady-state operating conditions. To investigate potential improvement in clearances a number of transient test runs were also made. They included engine power throttle bursts and chops and also hot rotor power throttle reburst.

3.0 BACKGROUND

Compressor airfoil tip clearance degradation (increased clearances) in revenue service engines is produced by causes related to engine operation and to shop maintenance practices. Of these, compressor stator casing out-of-roundness has been found to be one of the most significant causes of airfoil tip clearance degradation. The effect of casing out-of-roundness on compressor blade and vane clearances is illustrated in Figures 1 and 2, respectively.

To meet the minimum clearance at build-up, all blade tips have to be machined at least by the amount equal to the radial distortion, otherwise undesirable blade-to-casing rubs will occur. Vanes, on the other hand, only need to be machined in the area of the casing distortion.

The problem is aggravated because the effect of out-of-roundness on clearances is magnified for two reasons. First, by the permitted interchangeability of modules and, second, by the field shop practices at engine build-up. At every shop visit, the distorted casing may be matched with a different rotor thus causing shorter blades in it and ultimately in all engines of the fleet. Normal field shop practices during engine build-up require that the individual compressor rotor and stator casing modules be machined to provide a minimum clearance. Verification of the actual minimum clearance is accomplished by applying wax strips of known thickness to the stator casing and rotor spool lands and then installing the casing halves around the rotor. The rotor is then rotated through 360° after which the stator casing halves, upper and lower, are removed and the wax strip thicknesses are measured. If the wax strips were rubbed, indicating below minimum clearance, the airfoil tips are hand-ground to correct this condition. How the magnifying effect on clearances is produced is illustrated by the following specific field engine incident. Because an engine failed to meet the minimum performance standards it was disassembled and inspected to determine the causes. Inspection of the compressor indicated a large out-of-roundness in the stator casing, shown in Figure 3. Because of this casing condition clearances were below the minimum, requiring blade tip rework which was done with hand grinding tools. Consequently, much more of the blade tip was removed than was necessary. The casing out-of-roundness in this compressor, referred to as module A, was a maximum of 0.5 mm (20 mils) but the blade tips were up to 1.0 mm (40 mils) shorter at the leading and trailing edges. A typical blade tip profile from this compressor is compared with a machine ground blade tip from another compressor in Figure 4. To avoid this large performance penalty, revised field procedures have been specified for the repair of casing-out-of-roundness.

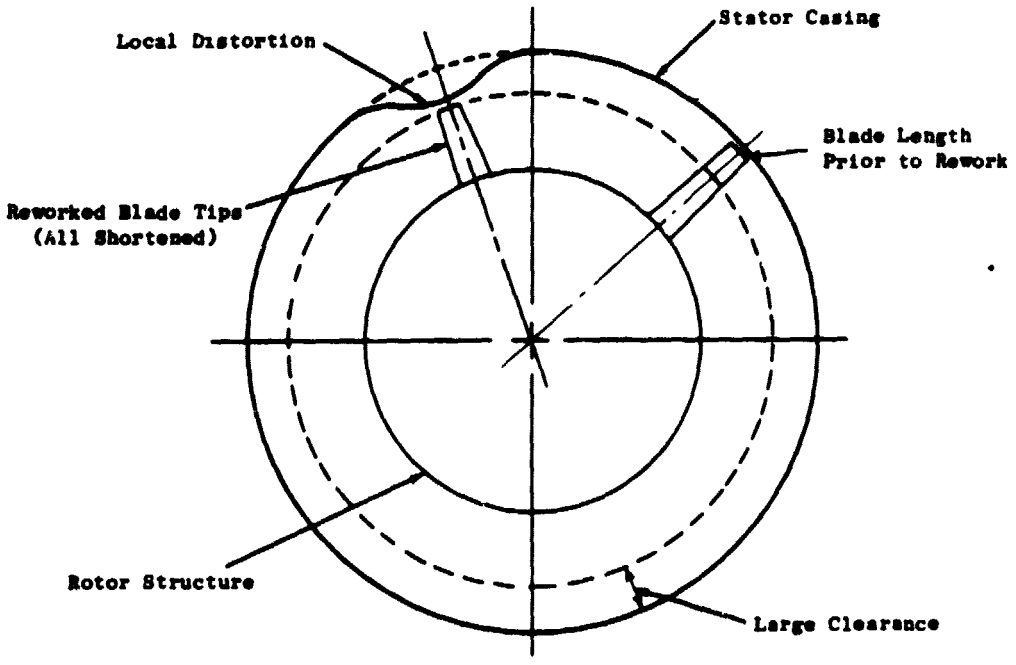

Figure 1. Casing Distortion Necessitates Rework on All Blade Tips in a Stage.

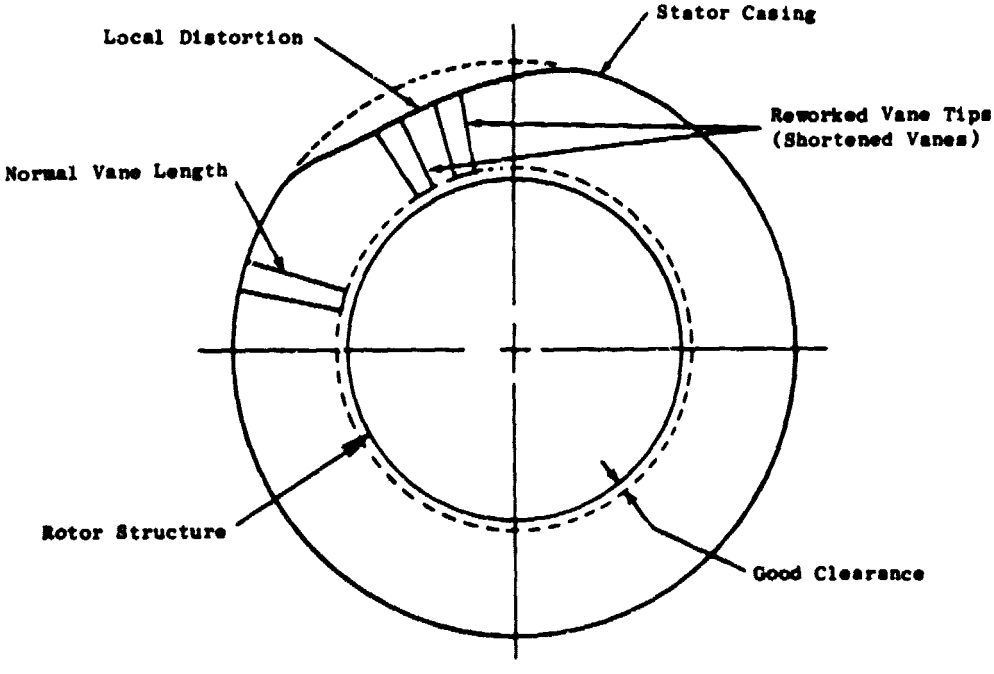

Figure 2. Casing Distortion Necessitates Rework on Vane Tips in Distorted Area Only.

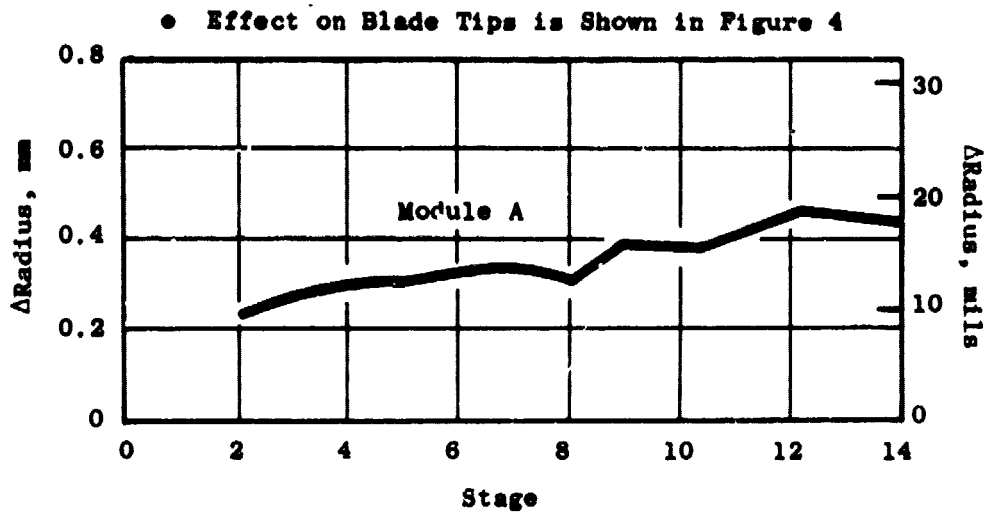

Figure 3. Casing Out-of-Roundness Versus Stage.

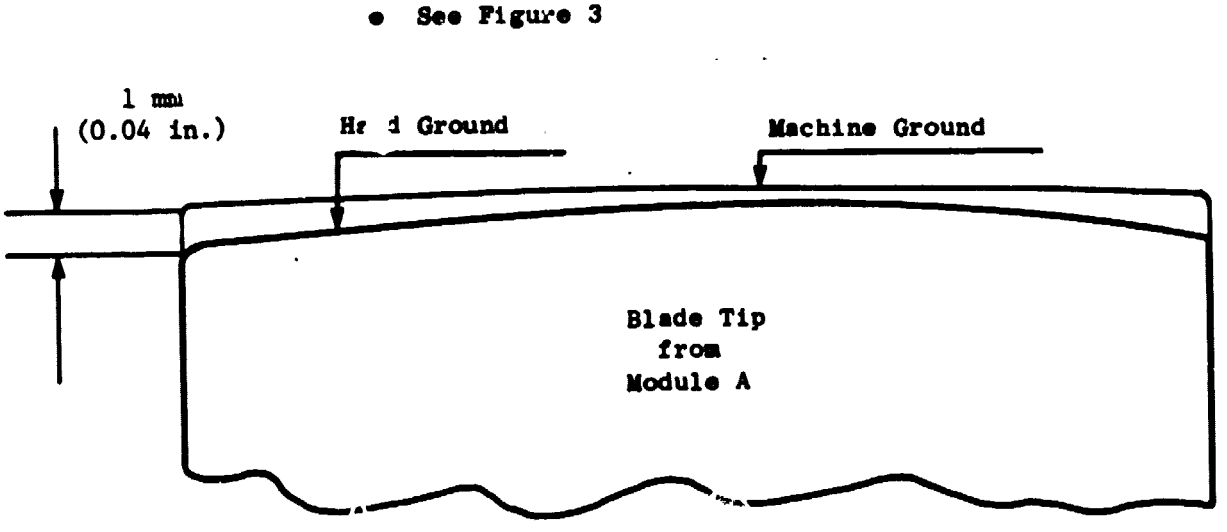

Figure 4. Because of Casing Out-of-Roundness, Hand Grinding of Blade Tips at Assembly Produces Shorter Blades than Necessary.

4.0 TEST APPARATUS

4.1 TEST FACILITY

The General Electric Evendale Altitude Test Facility was used for all testing reported here. The facility, shown in Figure 5, consists of six 10-stage axial-flow compressors, three LM1500 gas turbine drives, and two test sections, each 5.18 m (17 feet) in diameter and 17.07 m (56 feet) long. The facility supplied fan engine booster discharge conditions for both the simulated cruise and sea-level-static core engine inlet conditions. The required inlet air temperature was produced by compression and air pressure simulation was obtained by airflow throttling to achieve cruise and sea-level pressure levels. Ambient core engine inlet conditions were obtained with the facility compressors turned off and the engine drawing air from an ambient inlet stack.

4.2 TEST VEHICLE

The test vehicle used in this investigation was a CF6 core engine, specifically adapted to the Altitude Test Facility. CF6-50, CF6-80 and special slave hardware was used for this core engine test. An overall installation photograph is shown in Figure 6.

The core engine consisted of a 14-stage axial flow high pressure compressor (HPC), an annular combustor, and a two-stage high pressure turbine. A CF6-50 configuration fan module was modified for ducting shop air into the bore of the HPC rotor. Other modifications included a reworked inlet gearbox for slipring accommodation; elimination of the Nos. 1 and 2 bearings, which are present on fan engines; and installation of a 100-point slipring for compressor rotor instrumentation. The CF6-50 No. 3 bearing was retained for compressor rotor support.

The HPC rotor was of a CF6-80 configuration except for the Stage 1 and 2 disks, which were CF6-50 disks, modified to pass bore cooling air through the rotor forward shaft and disk hub area. The rotor blades were CF6-50 blades.

The HPC stator case was a CF6-80 configuration while the stator vanes were CF6-50 configuration. The CF6-50 stator casing is made in two pieces. The front casing is made from M152 steel and the rear casing is made from INCO 718. The CF6-80 stator casing is made in one piece from M152. In stages 12 through 14 the structure is insulated from the gas flow path. The combination of the lower coefficient of expansion of M152 and the insulation produce better-matched thermal responses of the rotor and stator than those in the CF6-50 compressor with an INCO 718 rear stator casing and uncooled rotor bore.

In this test program, externally supplied shop air was used to cool the rotor and thus vary the clearances. The total cooling airflow was measured by an instrumented orifice and was remotely controlled by a valve upstream of the orifice, shown in Figure 7. The cooling air was supplied to the manifold around the slave front frame; from there, through flexible hoses, into the frame struts and then into the HP compressor inlet inner cavity shown in Figure 8. From this

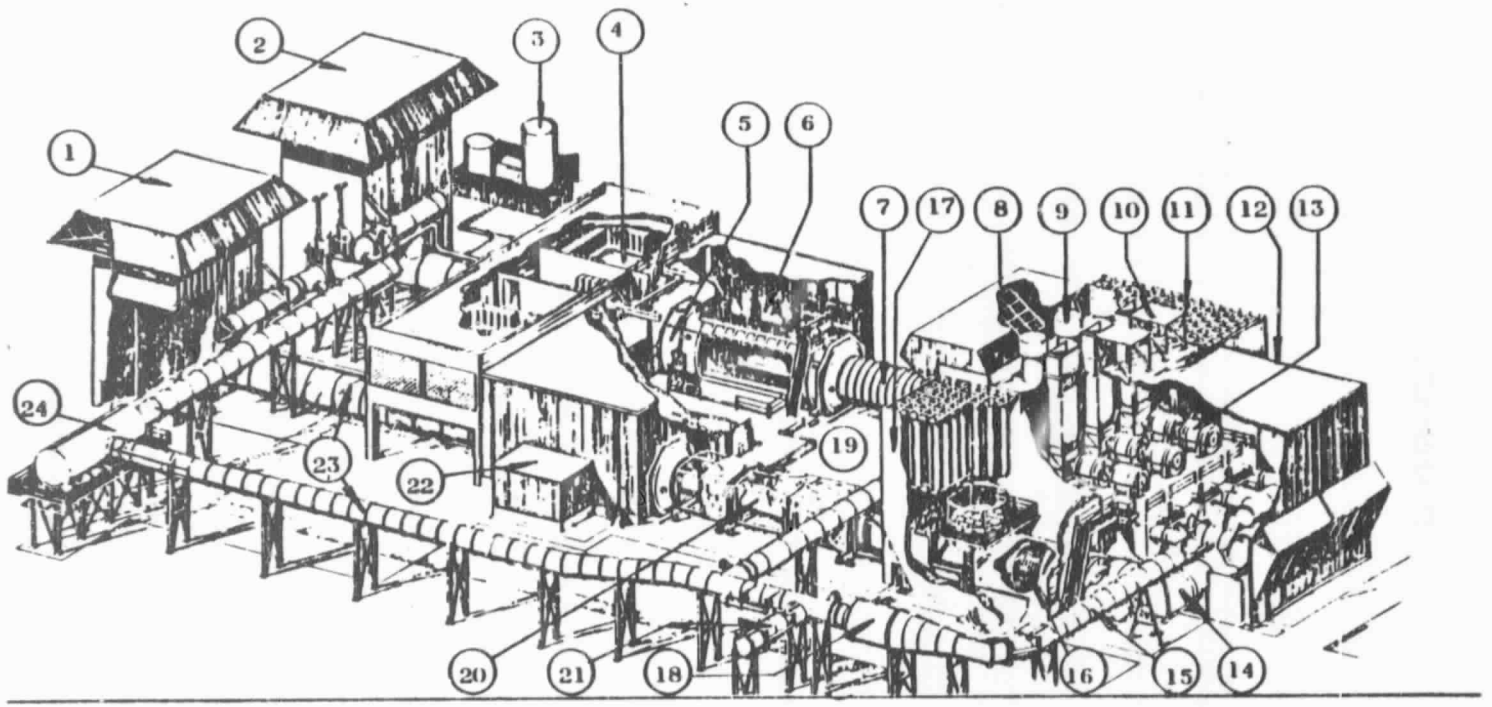

1. Inlet Stack No. 1, Cell 43
2. Inlet Stack No. 2, Cell 44
3. Liquid Air Supply
4. Control Rooms
5. Test Tank
6. Instrumentation Termination Panels
7. Augmenter Tube
8. Inlet Stack No. 3
9. Ventilation Fans
10. LM1500 Exhaust Stack and Cover
11. Exhaust Stack No. 2
12. Exhaust Valve for FS/5 Compressors
13. FS/5 Compressors
14. Engine Exhaust Inlet to LM1500 Driven FS/5 Compressor
15. FS/5 Discharge Duct
16. Water Separator
17. Exhaust Stack No. 1
18. After-Cooler
19. Location of Natural Gas Pumps and Barometric Well
20. Diffuser
21. XTF Inlet or Exhaust Plus 401 Air
22. Fuel Package Room
23. Inlet Duct
24. Air Heater

Figure 5. Evendale Altitude Test Facility.

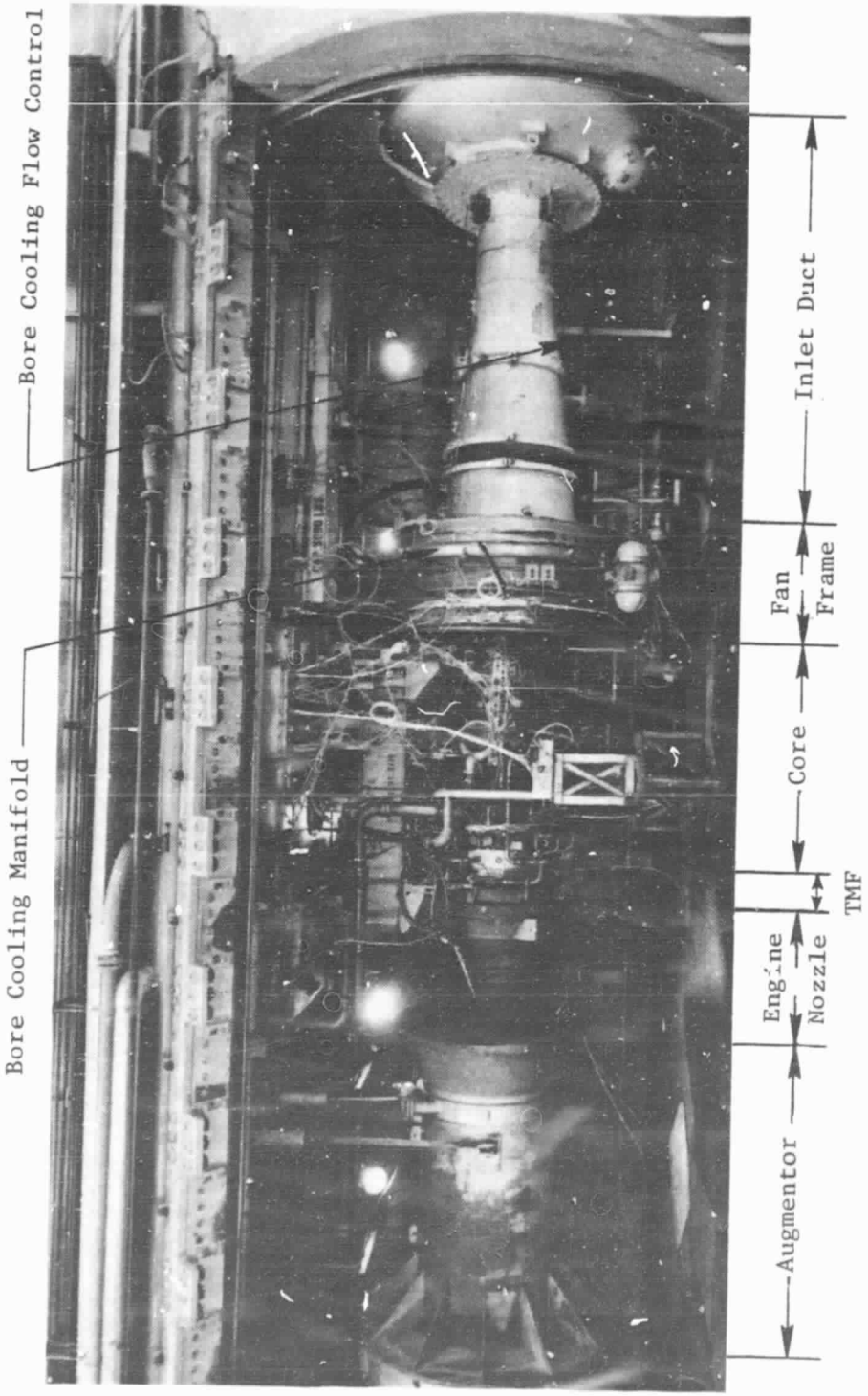

Figure 6. Engine Installation.

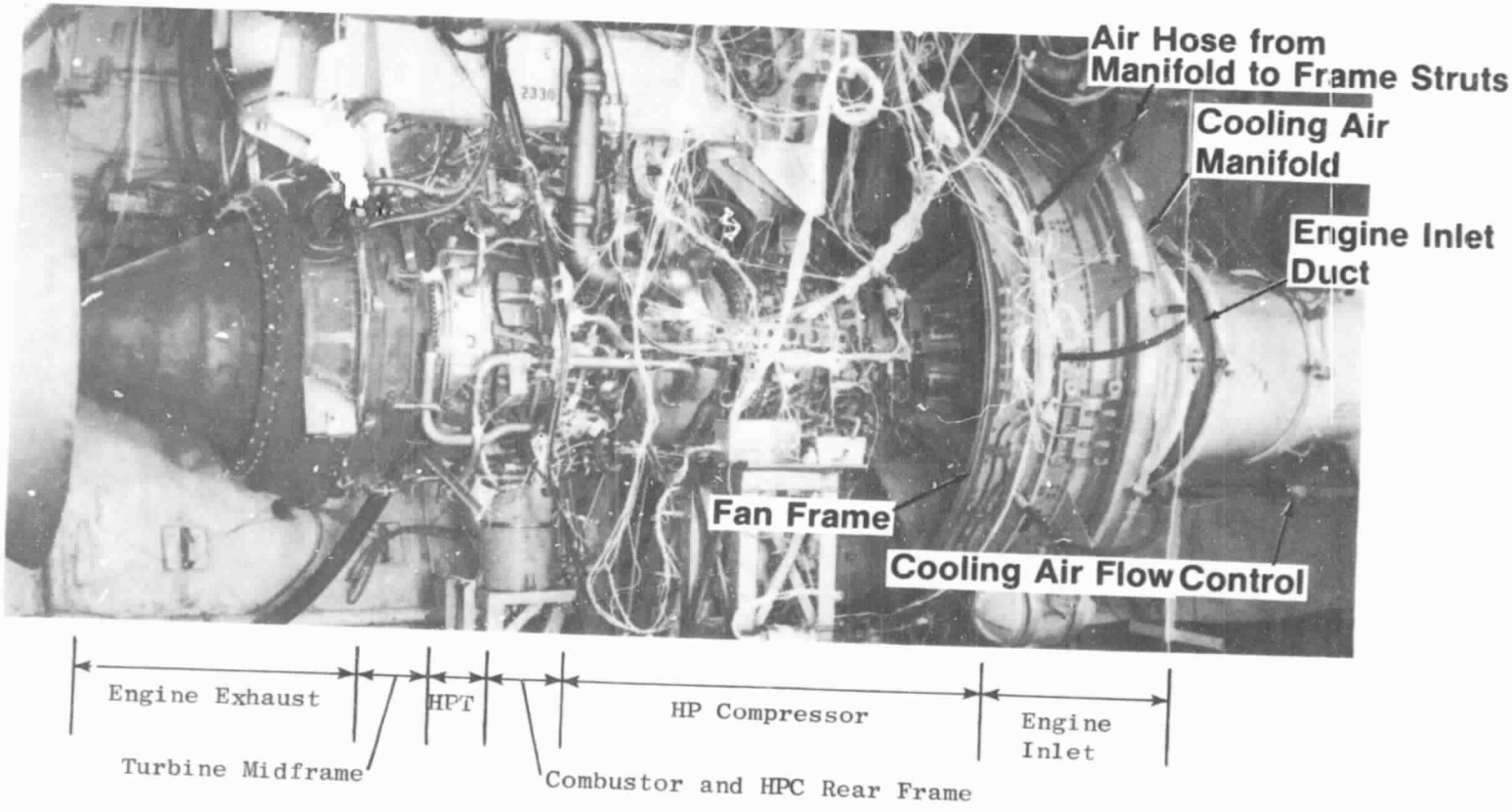

Figure 7. Instrumented Core Engine in Altitude Test Facility.

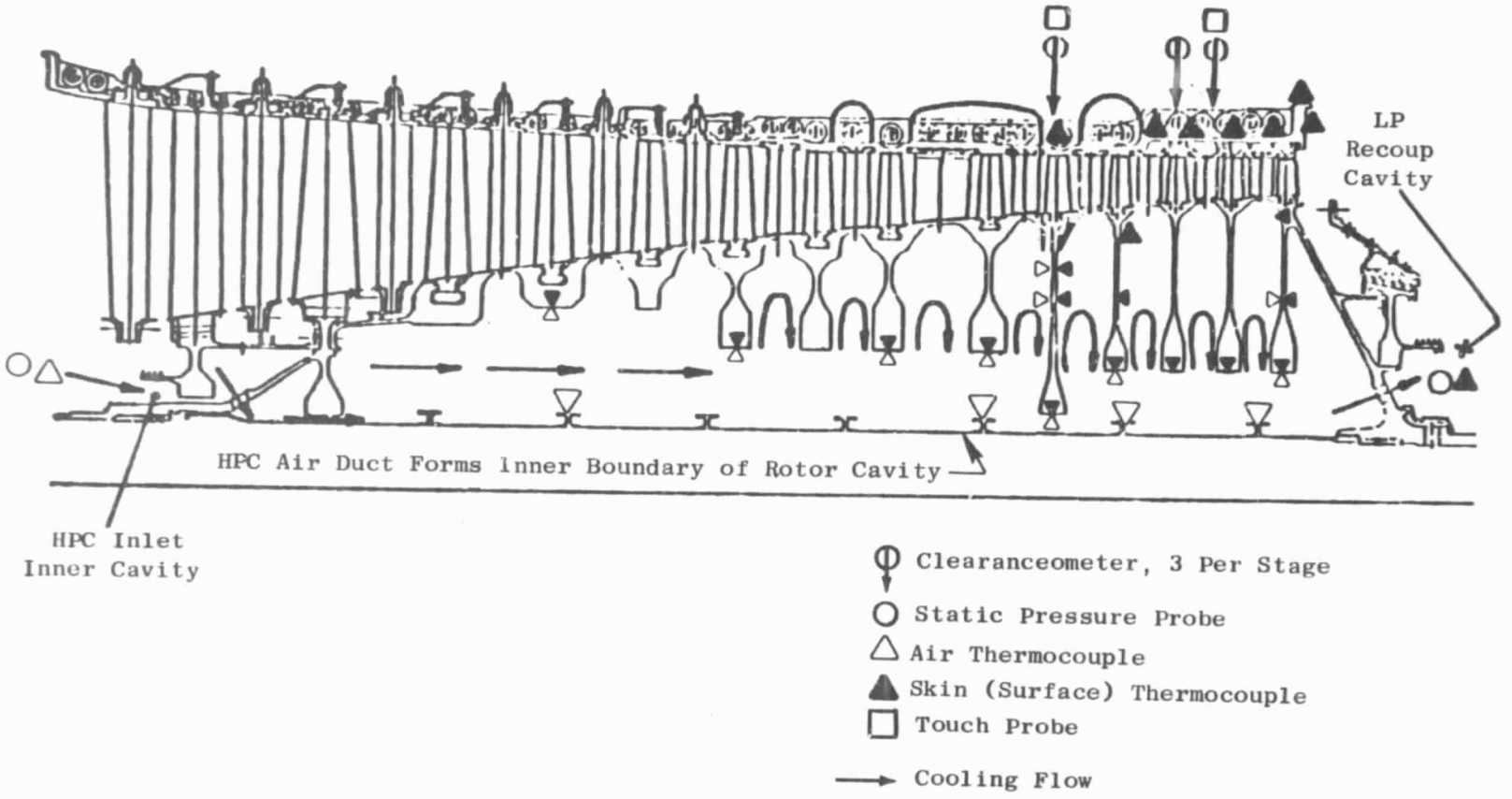

Figure 8. Compressor Instrumentation/Flow Schematic.

cavity, some of the air leaked out through the air/oil and air seals bounding the cavity (only the rotating seals are shown in the figure) and the remainder, the net cooling airflow, entered the rotor main cavity through the holes in the forward shaft. The cooling air exited the rotor cavity through holes in the rear shaft and was then vented through the compressor rear frame struts into the test facility exhaust.

4.3 INSTRUMENTATION

A detailed summary of instrumentation used is given in Appendix D. It consisted of the following three groups: 1) special instrumentation used for this investigation, 2) engine performance instrumentation, and 3) engine control and safety instrumentation.

Special instrumentation for this investigation is summarized in Figure 8 and it included a calibrated orifice to measure rotor bore cooling airflow, pressure and temperature probes at the rotor main cavity inlet and discharge for monitoring the cooling airflow conditions, compressor rotor and stator thermocouples, blade tip clearanceometers and touch probes.

The clearanceometers were electrical capacitance probes whose output voltage varied with the distance between the clearanceometers and the blade tips. Touch probes were traverse probes with open electrical circuits which closed when the probes touched the blade tips. When contact was made, the probes automatically backed off. The distance traversed by the probes, to touch the blade tips, was measured by linear potentiometers.

The engine performance instrumentation included pressure and temperature rakes at compressor inlet and discharge, exhaust gas temperature rakes and the engine pressure ratio rakes.

Engine control and safety instrumentation included a tachometer, a fuel flow meter and a variable vane position indicator.

The Automatic Data Handling (ADH) Computer system was used for data acquisition. Temperature data from the compressor rotor were acquired through a forward mounted slipring and programmed to the ADH computer. The compressor stator temperature data and the engine performance instrumentation data were programmed through junction boxes to the same computer system. The clearanceometers and touch probes were connected to the tape recorder and, in parallel, to the oscilloscopes for visual monitoring.

Engine control and safety instrumentation was programmed to the test cell control room where its output was displayed on the control console and monitored by the test crew. In addition, the output was displayed on strip charts and recorded by the ADH Computer system.

5.0 TEST PROCEDURE

A number of steady-state and transient engine test runs were made. They included steady-state power calibrations, power throttle bursts and chops, hot rotor power throttle rebursts and a simulated flight cycle test run.

The steady-state power calibration tests were made at constant speeds with three different engine inlet conditions, which were (1) core engine ambient, (2) simulated fan engine sea-level static and (3) cruise. At each engine speed point, at least three different sets of clearances were produced and their effects on engine performance were measured. The high pressure compressor airfoil tip clearances were varied by varying quantities of rotor bore cooling airflow. The greater the cooling airflow, at any power setting, the lower was the bulk temperature of the rotor structure and, hence, the greater were the tip clearances.

The test procedure for the steady-state power calibrations was as follows. After engine inlet conditions and speed were stabilized, the rotor bore cooling airflow was set at the desired level and, three minutes later, all instrumentation sensor outputs were scanned and recorded. Instrumentation output scanning and recording was repeated approximately every three minutes until the rotor disk temperatures became stable, which took fifteen to twenty minutes. At this point, the cooling airflow was changed and the instrumentation sensor output scanning and recording was repeated.

The power throttle bursts and chops were made with only the ambient engine inlet conditions because simulated fan engine compressor inlet temperatures and pressures cannot be rapidly produced when a core engine is run in an altitude test facility. The rotor bore cooling airflow was maintained at a constant fraction of the engine airflow. The power throttle bursts were made from ground idle to take-off power setting, which was then held constant until the rotor disk temperatures became stable and then the engine power throttle was chopped back to the ground idle setting.

A "hot rotor power throttle reburst" is defined as an engine power throttle chop from a high to a low power setting followed by a reburst to the high power setting. This type of power throttle maneuver may cause heavy airfoil tip rubs and thus increase the clearances for subsequent operation. This may be particularly so if the dwell time at the low power setting is of such a time period so as to produce the maximum temperature difference between the rotor and stator structures. In the hot rotor power throttle reburst tests the metal temperatures were stabilized at takeoff power setting and then the throttle was chopped to ground idle and, a short time later, reburst to takeoff power setting. Time at ground idle setting varied from 20 seconds to about 30 minutes. These tests were also run with ambient engine inlet conditions. The cooling airflow was maintained at a constant fraction of the engine airflow.

In all transient tests the transient data recording equipment was switched-on one minute before the power throttle movement was initiated and generally remained on for at least two minutes and, in some special cases, up to seven minutes after which time the steady-state data recording equipment was switched-on.

The parameters measured or determined included rotor bore cooling airflow, cooling air temperature inside the rotor cavity, compressor airfoil tip clearances, rotor and stator structure temperature, compressor efficiency and engine fuel flow. The total cooling airflow was measured by a calibrated orifice. The net rotor bore cooling airflow was obtained by calculating the leakage through the seals bounding the compressor inlet inner cavity, and then subtracting it from the total flow. The calculation method is discussed in the Section 6.0.

The airfoil tip clearance changes, at various rates of rotor bore cooling airflow, were calculated based on measured rotor disk temperatures. The calculated clearance changes in stages 10, 12, and 13 were verified by clearanceometer measurements. The calculation method is discussed in the Section 6.0.

The compressor efficiency changes produced by the compressor airfoil clearance changes were computed automatically from the measured air temperatures and pressures at compressor inlet and discharge.

The fuel flow changes, caused by the compressor airfoil clearance changes, were measured directly.

6.0 RESULTS AND DISCUSSION

Results presented were obtained from the steady-state power calibrations and the transient test runs. They include rotor bore cooling airflow, rotor temperatures, compressor clearances, compressor efficiency and engine fuel flow. All the steady-state results presented are changes, in the measured or determined parameters, caused by varying the rotor bore cooling airflow; the results obtained at zero net rotor bore cooling airflow were used as the base line in the presentation.

6.1 STEADY-STATE RESULTS

Net Rotor Bore Cooling Airflow

At each steady-state power calibration speed point the total cooling airflow was reduced until the net flow through the compressor rotor cavity was zero as indicated by the temperature and pressure sensors at the inlet and discharge of the rotor cavity. It followed, therefore, that for this condition the leakage through the seals was equal to the total flow measured at the orifice. A leakage flow function was determined from this set of data and it was used to calculate leakage through the seals at the higher rates of the total cooling airflow. The net rotor bore cooling airflow was then obtained by subtracting leakage from the total measured flow. The net rotor bore cooling airflow function for all power calibration speed points is shown in Figure 9.

Rotor Temperature

The axial air temperature profiles measured at the inner boundary of the rotor cavity are shown in Figure 10 for various rates of cooling airflow. The data indicate a slower temperature increase in the middle stages (stage 4 through 9) than in the rear stages of the rotor structure. This is primarily due to the geometrical differences of these two areas of the rotor structure and, to some small extent, due to the higher conductivity of INCO 718 (rear stages) as compared to titanium (forward stages). The data also show, as would be expected, that the higher the cooling airflow the lower the air temperature of the rotor cavity.

Disk bore metal temperatures are shown in Figure 11 for various rates of rotor bore cooling airflow. These data also show that the greater the cooling airflow the lower are the disk bore temperatures. At stage 14, the maximum cooling airflow reduced the metal temperatures by about 170°C (300°F) which is a very significant reduction.

Radial temperature profiles in the stage 14 disk are shown in Figure 12. The cooling air was most effective at the disk bore. The rim of the disk was much less affected and the maximum temperature reduction was about one quarter of that at the bore. In other stages, this was even a smaller fraction. As will be noted from the figure, the effectiveness of rotor bore cooling was significantly underestimated when the pre-test predictions were made.

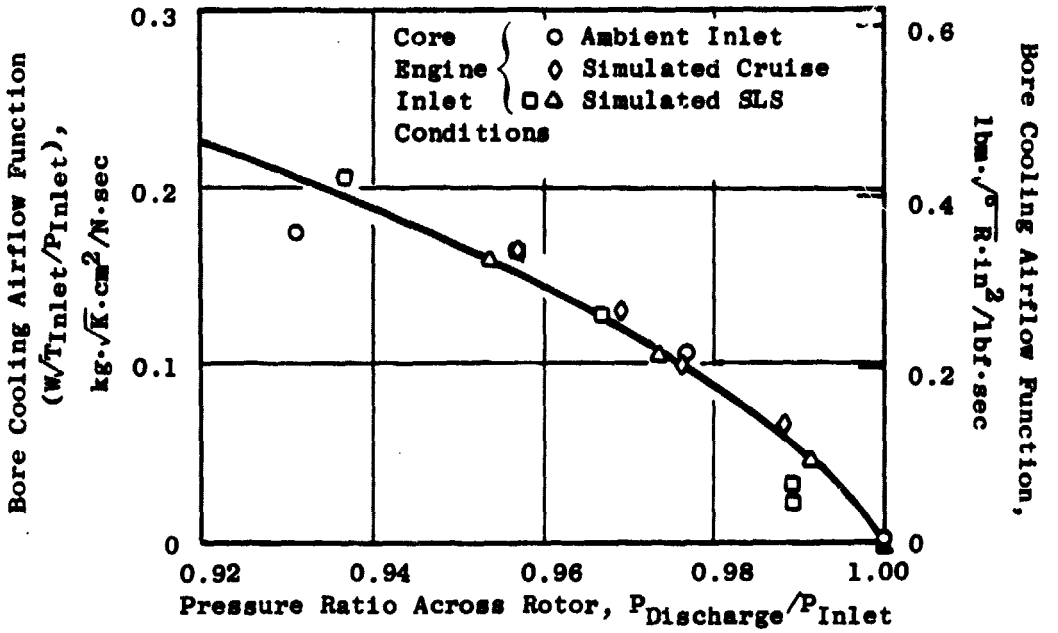

Figure 9. Rotor Bore Cooling Airflow Function for the Steady-State Power Calibration Speed Points.

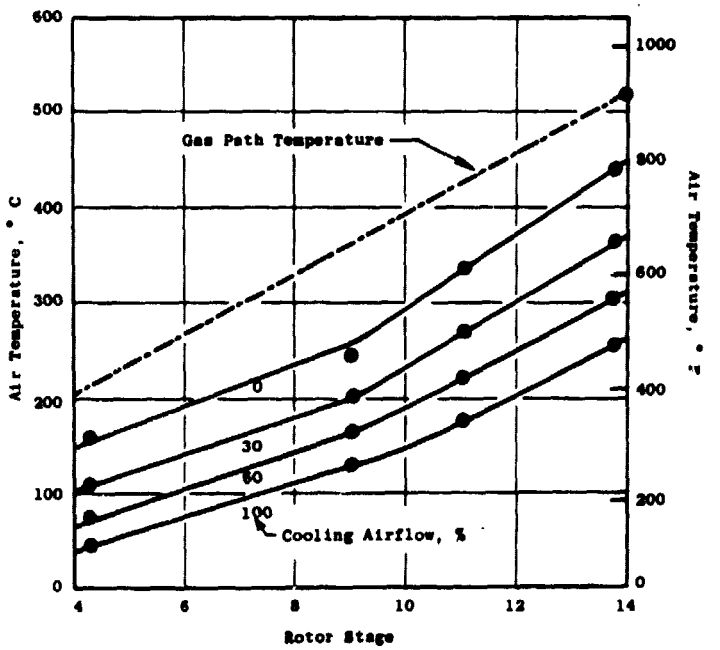

Figure 10. Air Temperatures at Rotor Inner Diameter for Various Cooling Airflow Rates.

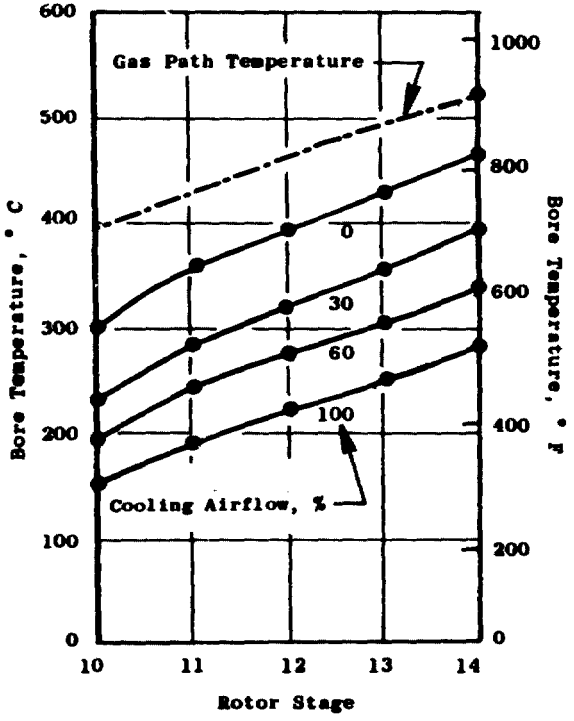

Figure 11. Disk Bore Temperatures at Various Cooling Airflow Rates.

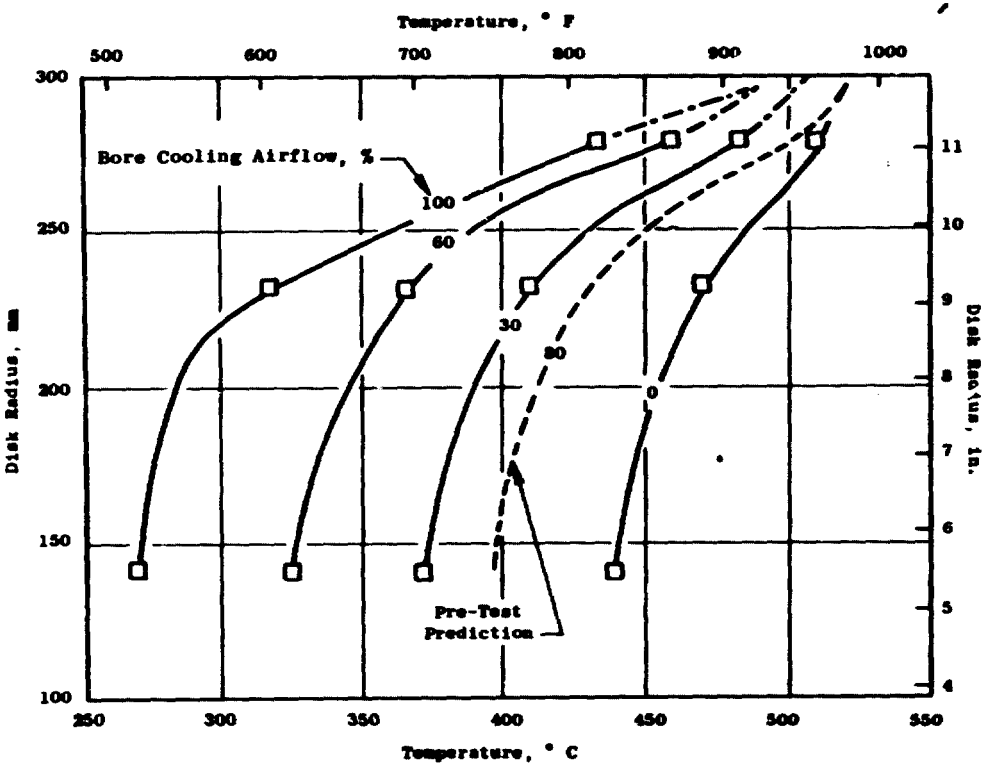

Figure 12. Radial Temperature Profiles in Stage 14 Disk at Various Cooling Airflow Rates.

Airfoil Tip Clearance Changes

At the power calibration points, the stator casing temperatures remained constant, and only the rotor temperatures were affected by the cooling airflow. Therefore, to calculate the clearance changes only the rotor temperature changes were needed to be considered. Clearance changes, calculated in this manner for the simulated sea level static takeoff power calibration point, are shown in Figure 13 for various cooling airflow rates. The data show that the greatest increase in clearances, produced by increased cooling airflow, occurred in the aft stages (stage 10 through 14). This is so because of the faster heat removal from these stages, as indicated by a faster cooling air temperature rise shown in Figure 10 and also because of the higher thermal coefficient of expansion of the disk material (INCO 718) in these stages than that in the forward and middle stages (titanium).

Similar calculations of clearance changes were made for other power calibration points. These data were then used to calculate the normalized average clearance changes which were later correlated with the corresponding compressor efficiency and engine fuel flow changes. The correlations are discussed in a later paragraph where the normalized average clearance is also defined.

The measured and calculated clearances for stages 10, 12 and 13 are shown in Figures 14 through 16. There is an excellent agreement for stage 10. For the other two stages, there are small discrepancies between measured and calculated data. The calculated data are somewhat lower. For instance, for a measured change of 0.76 mm (30 mils) the corresponding calculated value is 0.63 mm (25 mils) or 0.13 mm (5 mils) less.

Efficiency and Fuel Flow Changes

Compressor efficiency changes resulting from variations of cooling airflow rates are shown in Figure 17. The data were obtained at the simulated sea-level static takeoff condition. Indicated and corrected values are shown in the figure. The corrections were made to obtain the net effect of clearance changes by allowing for the leakage of cooling air into the compressor inlet and for the heat removal, by the cooling air, from the compressor gas path.

The magnitude of the correction for heat removal was about ten times as large as that for leakage. The corrections were necessary because an increased rotor bore cooling airflow produced an increased leakage of the cooling air into the compressor inlet downstream of the inlet temperature rakes. Because the cooling air was colder than the air at the compressor inlet, the resultant air temperature of the mixed air was slightly lower than measured by the inlet temperature rakes. The air temperature rise through the compressor, as measured by the inlet and discharge rakes was, therefore, slightly smaller than the actual. Consequently the computed (indicated) efficiency reduction, based on the measured temperature rise, was also slightly smaller than the actual efficiency reduction. Similarly, the heat removed from the gas path by the increased cooling airflow reduced the indicated air temperature at compressor discharge and, hence, made the indicated temperature rise through the compressor slightly smaller than the actual. Consequently, the computed efficiency reduction, due to the increased cooling airflow, was also slightly smaller than the actual.

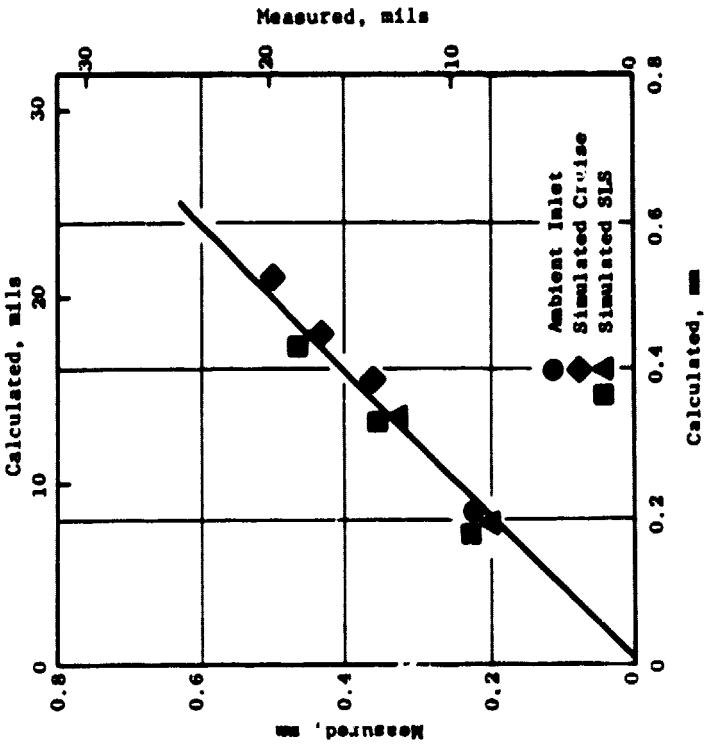

Figure 14. Stage 10 Airfoil Tip Clearance Changes, Measured Versus Calculated.

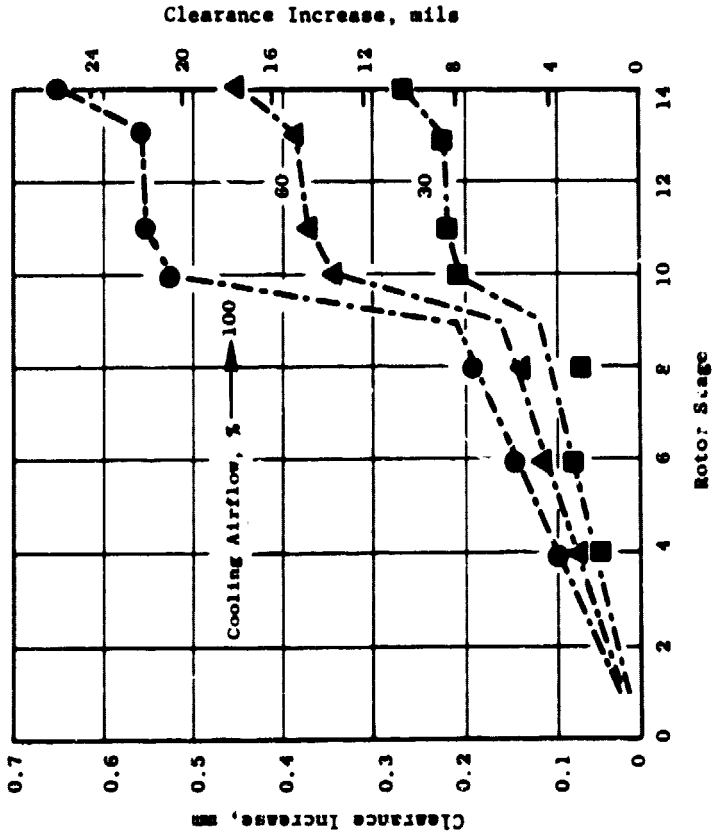

Figure 13. Calculated Airfoil Tip Clearance Changes for Various Cooling Airflow Rates.

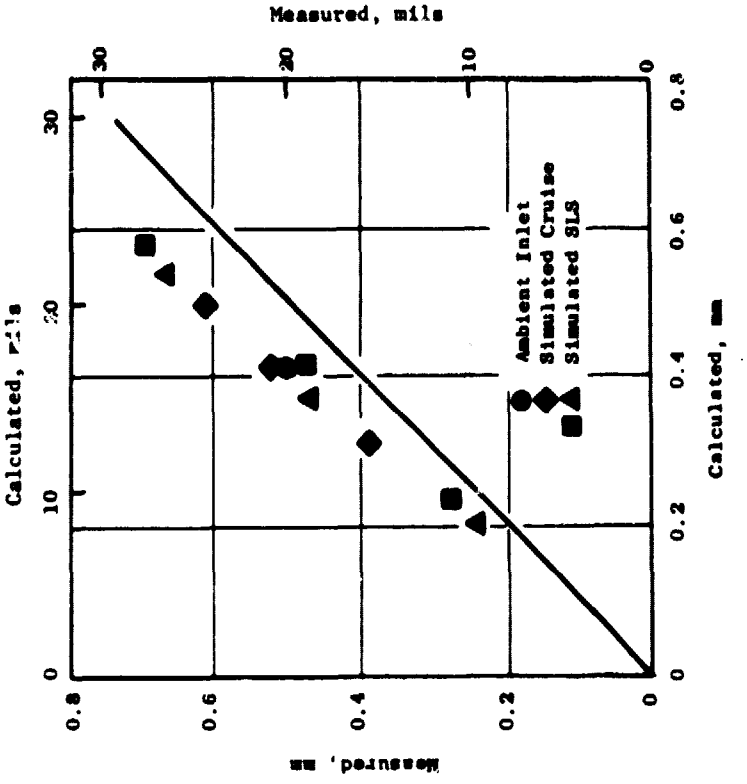

Figure 16. Stage 13 Airfoil Tip Clearance Changes, Measured Versus Calculated.

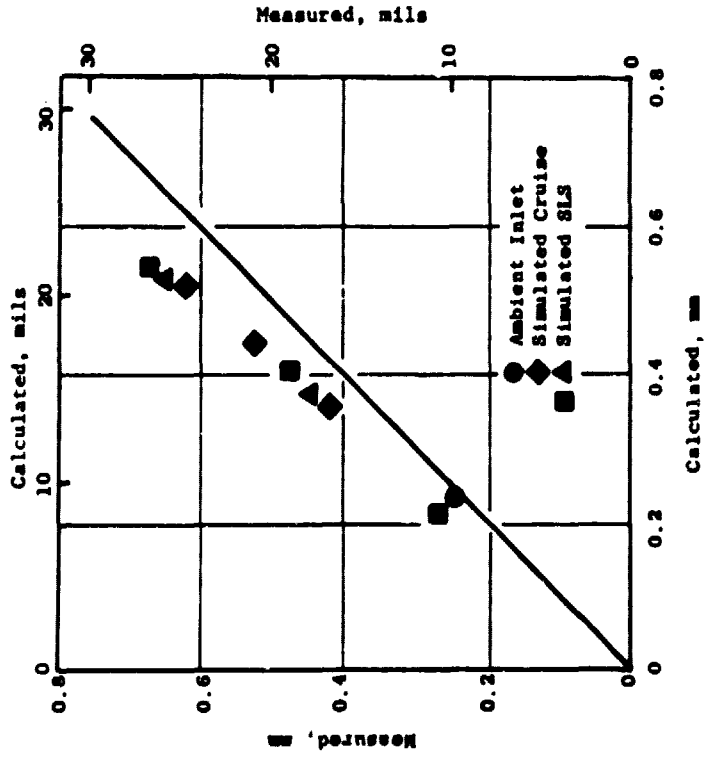

Figure 15. Stage 12 Airfoil Tip Clearance Changes, Measured Versus Calculated.

Engine fuel flow changes as a function of the cooling airflow are shown in Figure 18. The corrections made to the fuel flow rate were in the opposite direction to that of the efficiency corrections, i.e., the fuel flow corrections resulted in a smaller actual fuel flow change than indicated, because the measured fuel flow included the energy removed from the cycle by the cooling air which was vented overboard. If the clearance changes were produced mechanically there would be no heat loss from the cycle and, therefore, the total fuel required would be less.

The compressor efficiency and fuel flow changes were corrected in this manner for all power calibration speed points and then correlated with the average normalized clearance changes as discussed in the next paragraph.

Correlation of Efficiency and Fuel Flow Changes with Clearance Changes

Compressor efficiency changes are shown as a function of the normalized average clearance changes in Figure 19 for four different speed points and three different engine inlet conditions. There is a good correlation of measured efficiency changes with the calculated normalized average clearance changes. The normalized average clearance change is defined as follows:

$$\overline{\Delta(CL/L)} = \frac{1}{N} \sum_{i=1}^{n} 0.5 \left[(\Delta CL/L)_r + (\Delta CL/L)_s \right]_i$$

ΔCL is clearance change in a given stage,
L is airfoil length in the same stage,
N is number of stages in the compressor,
n is number of stages in which clearance is changed,
r denotes rotor,
s denotes stator.

$\overline{\Delta CL/L} \times 100$ is colloquially referred to as "percent of clearance change" instead of "average normalized clearance change in percent of the airfoil length".

The line shown in the figure is drawn by inspection through the data points and it happens to be a 45° line, indicating that one percent of the normalized average clearance change produces also a one percent change in the compressor efficiency.

The engine fuel flow changes versus the normalized average clearance changes are shown in Figure 20. Only the data obtained at the simulated sea level static takeoff and cruise conditions are presented. The data for the other two speed points were inaccurate because of a fuel flow meter malfunction. The line shown in the figure is derived from the efficiency line in Figure 19 through the derivative of fuel flow as a function of efficiency for the test engine. Because the line correlates well with the fuel flow data it indicates consistency of the measured efficiency and fuel flow changes.

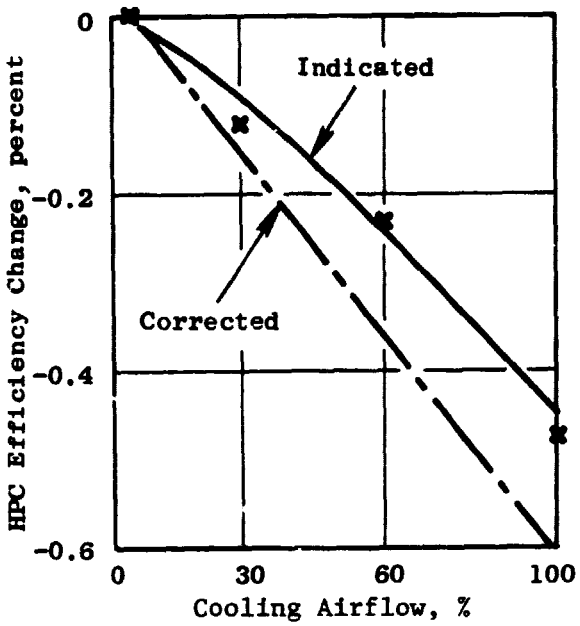

Figure 17. HPC Efficiency Change Versus Bore Cooling Airflow.

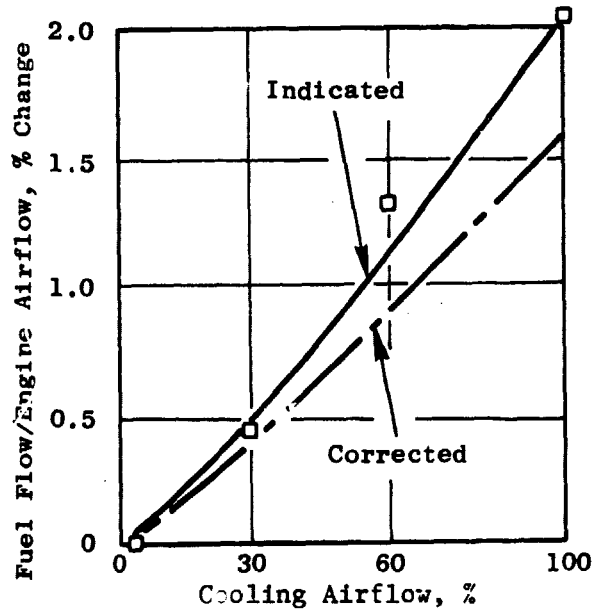

Figure 18. Fuel Flow Change Versus Bore Cooling Airflow.

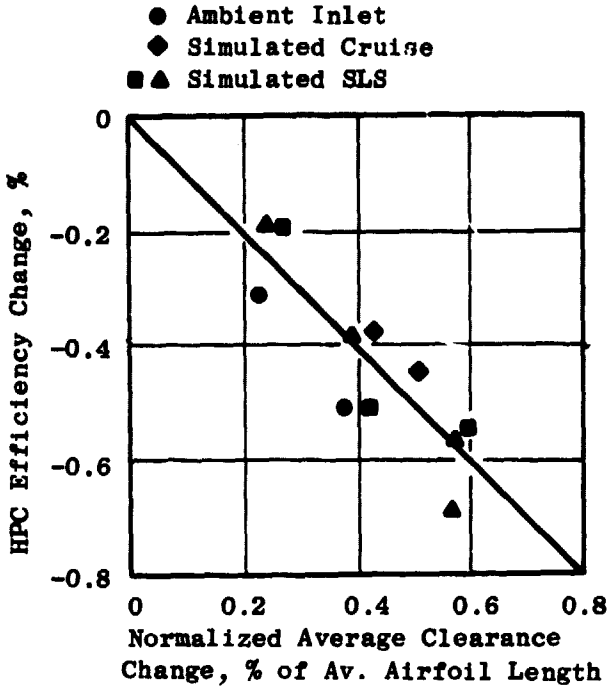

Figure 19. Compressor Efficiency Change Versus Airfoil Tip Clearance Change.

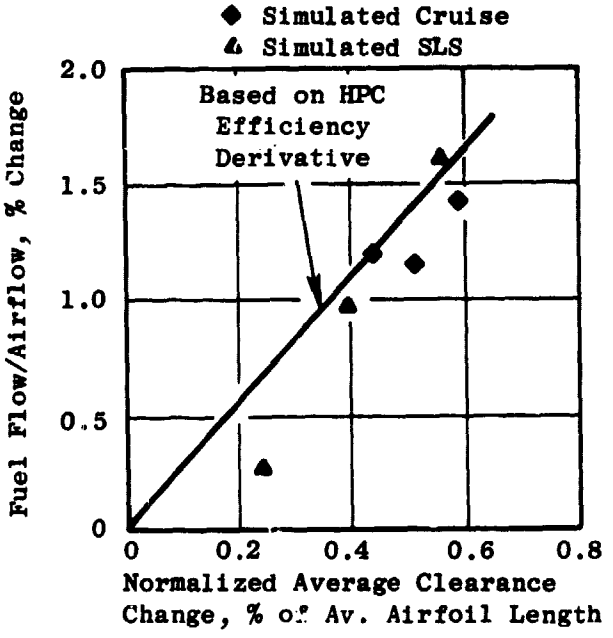

Figure 20. Fuel Flow Change Versus Airfoil Tip Clearance Change.

6.2 TRANSIENT RESULTS

Clearance Changes During Power Throttle Bursts and Chops

In these tests the engine power throttle was burst from ground idle to takeoff power setting and held there until the compressor metal temperatures, and hence, airfoil tip clearances, stabilized. The measured clearance change for the stage 10 blades is shown in Figure 21. The total clearance change measured in this test run was about 0.25 mm (10 mils). After the steady-state temperatures and clearances at take-off power had been reached, the engine power throttle was chopped to ground idle setting and held there until the metal temperatures and clearances stabilized again. The measured clearances in stage 10 for this engine power maneuver are shown in Figure 22 where the total clearance change is less than 0.38 mm (15 mils). Clearance variations measured in stages 12 and 13 were similar and are shown in Figures 23 through 25.

Comparison of Measured and Calculated Clearances

The blade tip clearances measured in stage 13 during the burst and chop engine power throttle maneuvers are shown in Figures 26 and 27 respectively where they are compared to the predicted values. The values shown in these figures represent clearance changes and not the absolute clearances. These variations were produced by engine speed and temperature changes; the rotor bore cooling airflow was maintained constant at a preset fraction of the engine airflow. Two things are worthy of note: 1) All observed clearance changes caused by engine power throttle maneuvers were small; 2) there is an excellent correlation between the measured and calculated clearance changes.

Hot Rotor Power Throttle Rebursts

A number of hot rotor power throttle reburst test runs were made. In each run the compressor metal temperatures and hence clearances, were permitted to stabilize at the high power setting, the simulated takeoff, and then the engine power throttle was chopped to ground idle setting and held there for a period of time, which differed for each test run. After the hold period at idle the engine power throttle was reburst to the high power setting. The measured clearance changes in stages 10, 12 and 13 during two such test runs are shown in Figures 28 and 29. Figure 28 shows clearance changes for a reburst after a 20 seconds dwell at idle and similar results for a 90 seconds dwell at ground idle are shown in Figure 29. The biggest clearance change of about 0.5 mm (20 mils), was produced in stage 10 in a reburst after 90 seconds at ground idle. This is because the stage 10 casing is not insulated and therefore the rotor and stator thermal responses are not as well matched as those of the other two stages.

Clearance Change in a Typical Flight Mission

A simulated flight mission was also run with the ambient core engine inlet only, for the same reasons as previously stated for the power throttle burst and chop runs, i.e. inability to rapidly change the inlet temperatures

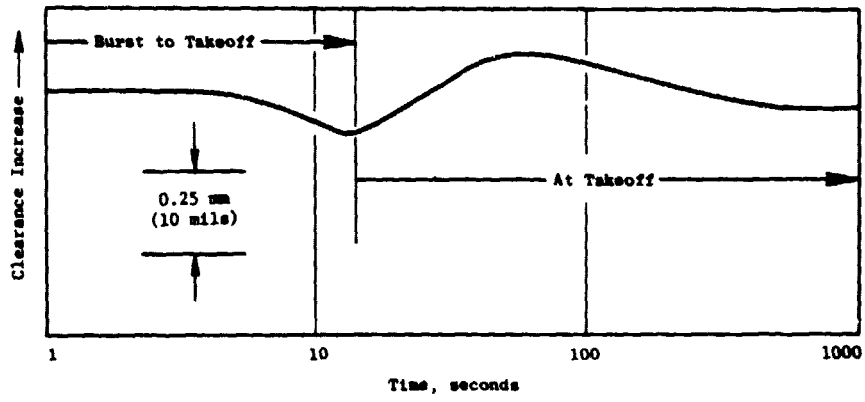

Figure 21. Small Variation of Clearance in Stage 10 After Power-Throttle Burst from Ground Idle to Takeoff.

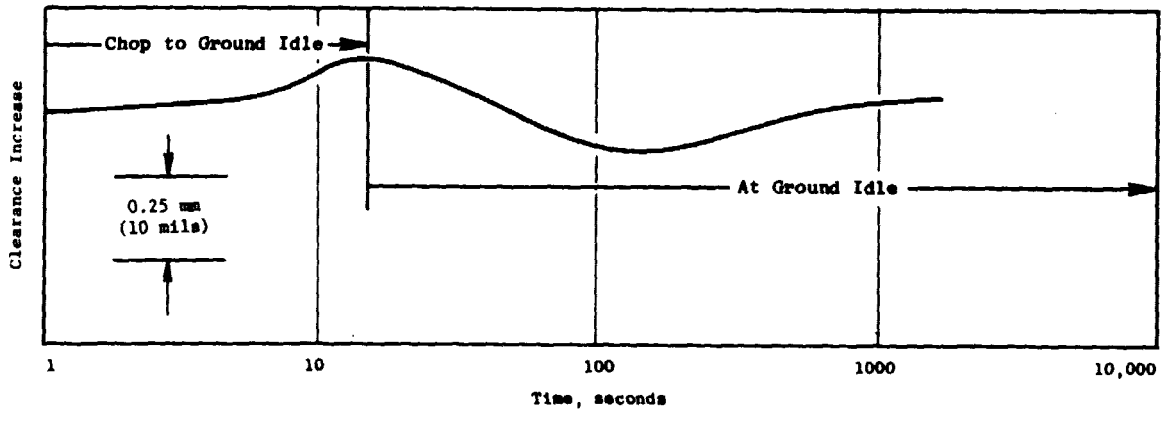

Figure 22. Small Variation of Clearance in Stage 10 After Power-Throttle Chop from Takeoff to Ground Idle.

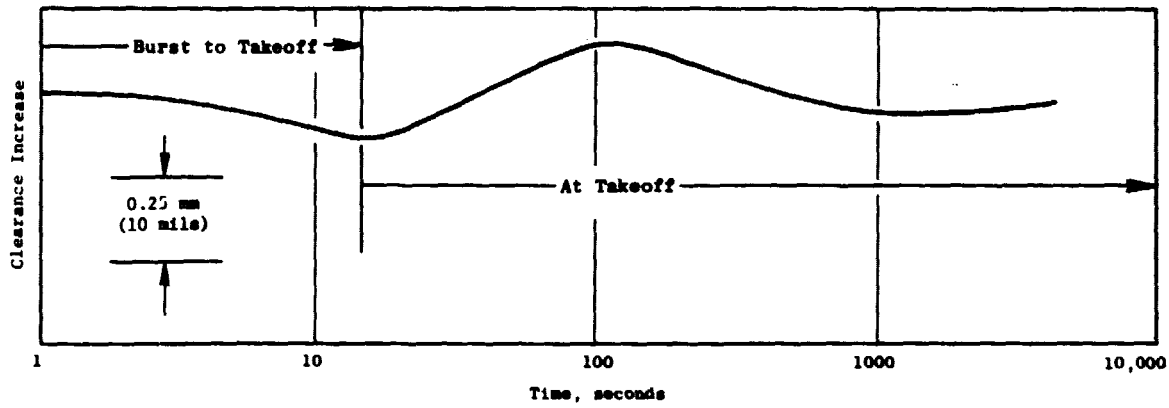

Figure 23. Small Variation of Clearance in Stage 12 After Power-Throttle Burst from Ground Idle to Takeoff.

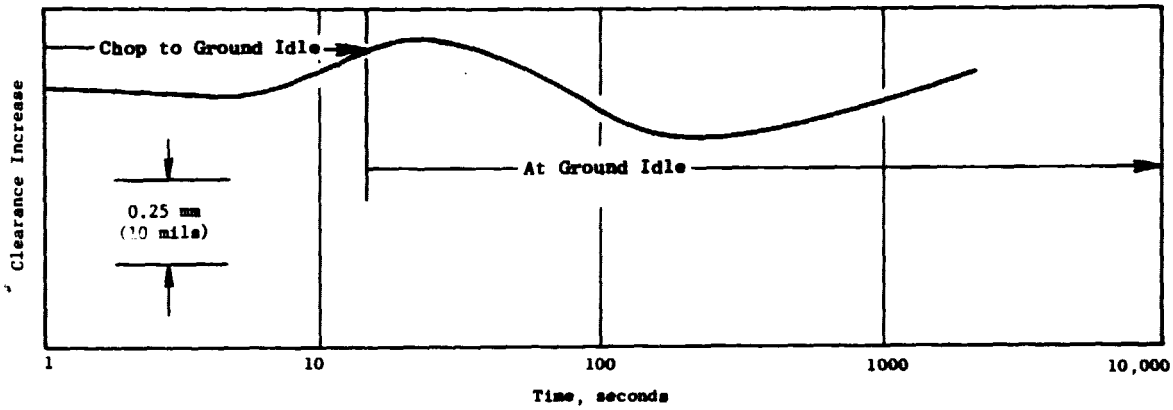

Figure 24. Small Variation of Clearance in Stage 12 After Power-Throttle Chop from Takeoff to Ground Idle.

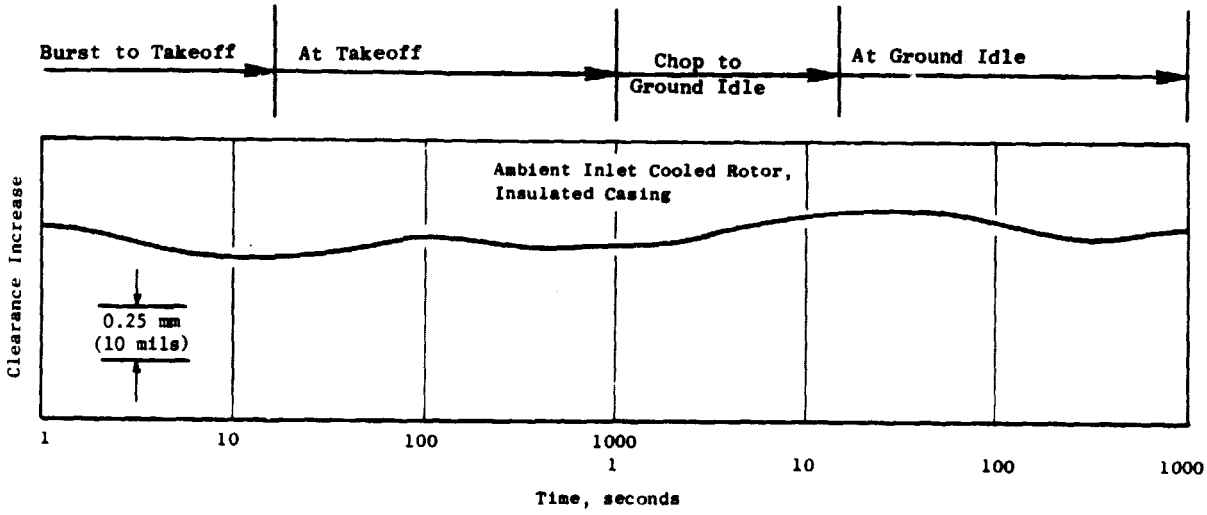

Figure 25. Small Variation of Clearance in Stage 13 After Burst and Chop Power-Throttle Movements.

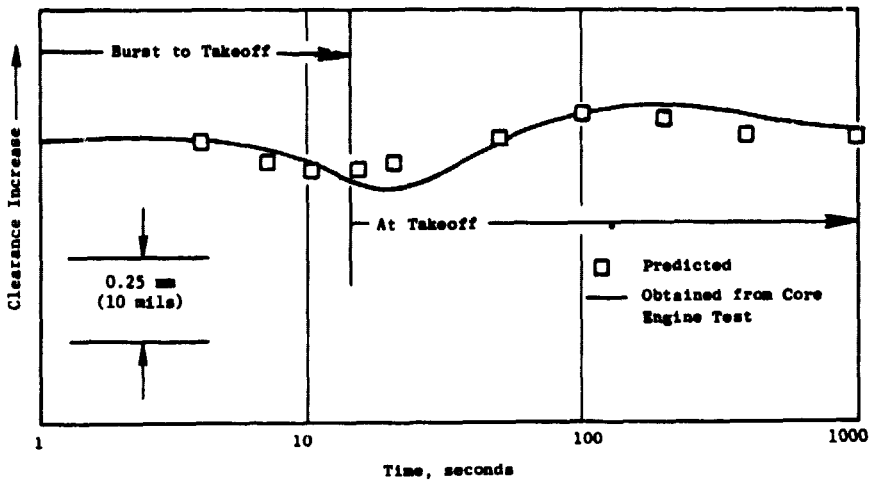

Figure 26. Small Variation of Clearance in Stage 13 After Power-Throttle Burst from Ground Idle to Takeoff.

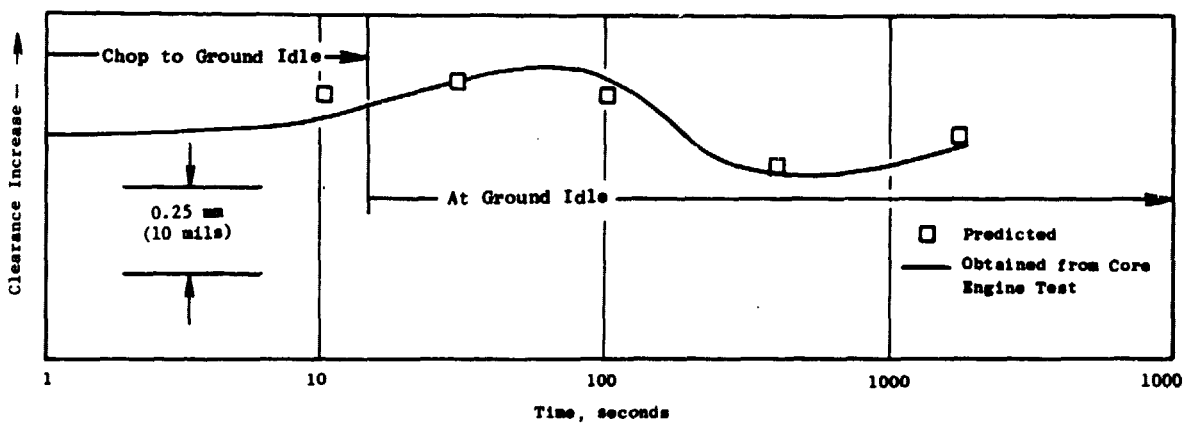

Figure 27. Small Variation of Clearance in Stage 13 After Power-Throttle Chop from Takeoff to Ground Idle.

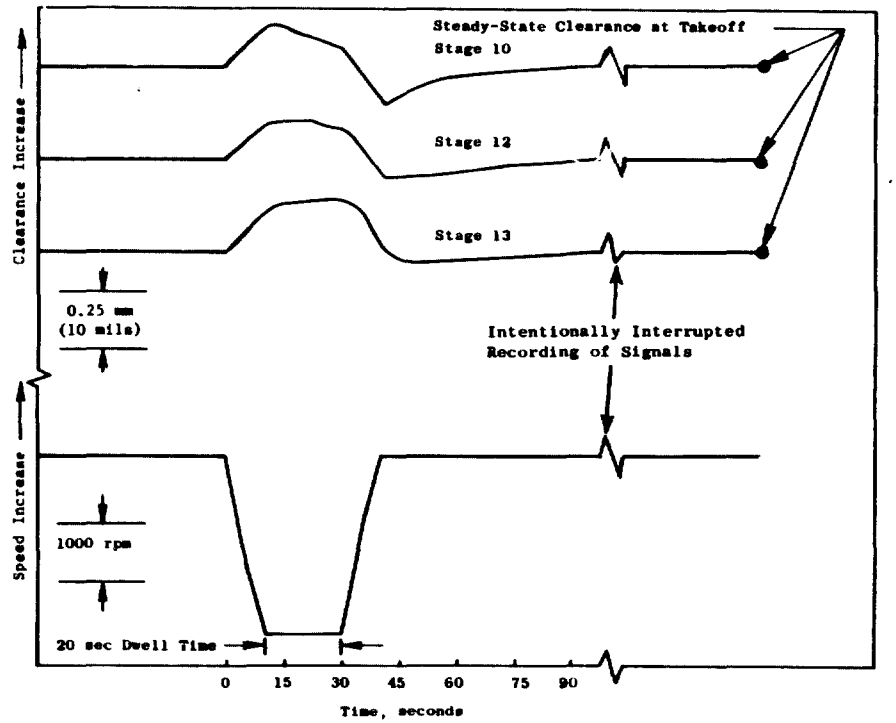

Figure 28. Small Variation of Clearance in a Hot Rotor Power-Throttle Reburst, 20-Second Dwell Time.

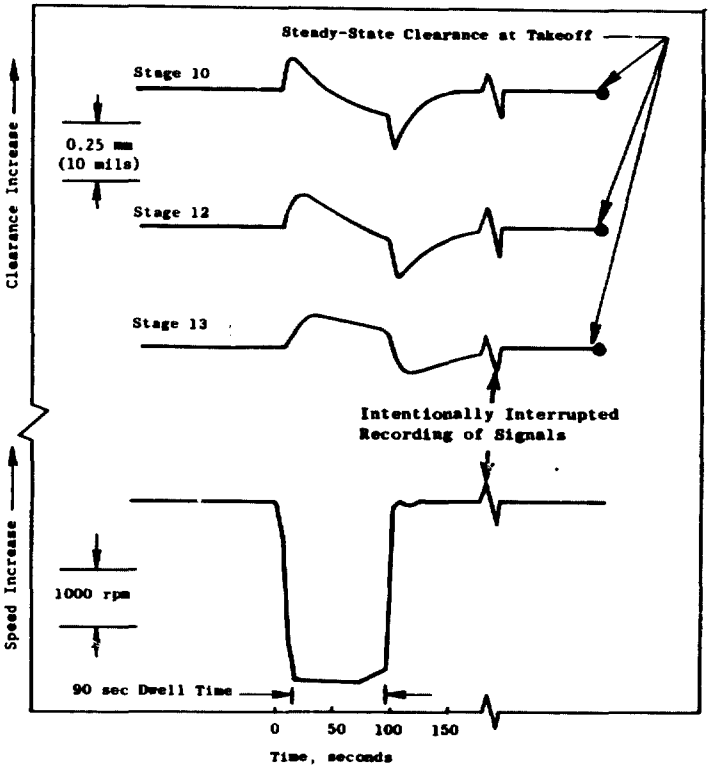

Figure 29. Small Variation of Clearance in a Hot Rotor Power-Throttle Reburst, 90-Second Dwell Time.

and pressures in the altitude test facility. Clearance changes measured in stages 10, 12 and 13 are shown in Figures 30 through 32. In this test the variations in clearances were also produced by changes in engine speed and temperature; the rotor bore cooling was maintained constant at a preset fraction of the engine airflow as was the case in the burst and chop tests. The measured clearance changes are also comparable to those measured during power throttle burst and chop tests.

Improved Clearances

At the steady-state power calibrations the rotor bore cooling was varied from test-point-to-test-point and was used as a means of varying the airfoil tip clearances to determine the effect of these variations on the compressor efficiency and on the engine fuel consumption. During the transient testing the rotor bore cooling was maintained constant at a preset fraction of the engine airflow, as would be the case in a fan engine. This was done to obtain better-matched thermal responses of the rotor and stator structures than those of the CF6-50 compressor. The results obtained from the transient tests are summarized in Figure 33 which shows clearance variation in a typical power throttle maneuver which included burst to takeoff, steady-state at takeoff and chop to ground idle. Figure 34 shows calculated clearance variations during a similar power throttle maneuver for the CF6-50 compressor i.e. for an uninsulated INCO 718 stator casing and an uncooled rotor. It will be noticed that cooling of the rotor bore, insulating of the stator casing together with a smaller thermal coefficient of expansion of the casing, produces significantly reduced clearance variations during engine transients and, therefore, permits much smaller compressor buildup and running clearances. Calculations indicate that these clearances can be reduced by 1.0 mm (0.040 in) in the aft stages of the compressor relative to the current CF6-50 compressor clearances. One mm (.04 in) reduced clearances in stages 10 through 14 would produce a reduction of 0.78 percent in the average normalized clearance.

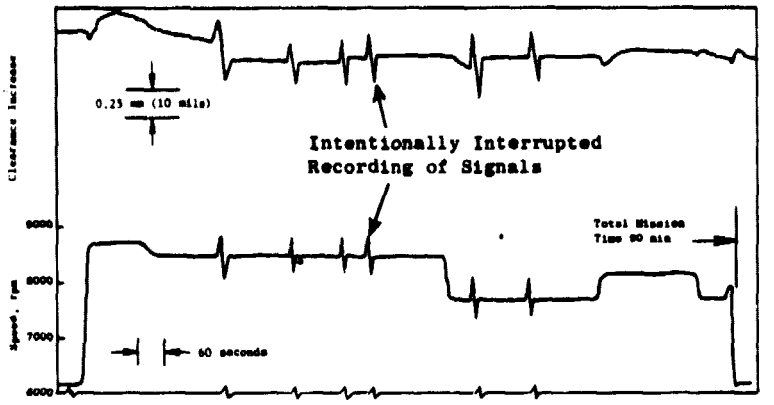

Figure 30. Small Variation of Stage 10 Blade Tip Clearance in a Simulated Typical Flight Mission.

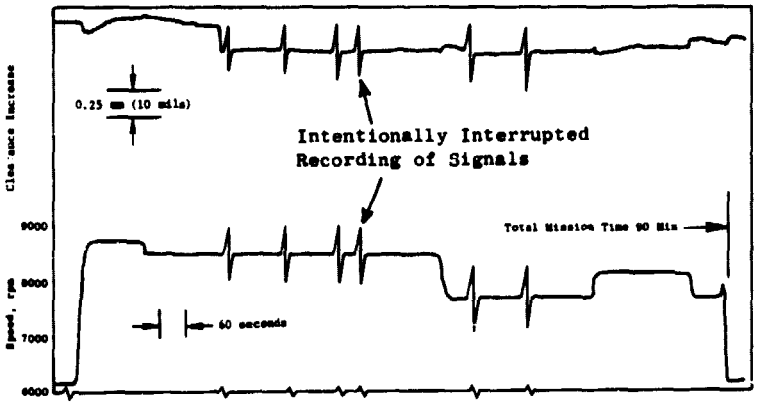

Figure 31. Small Variation of Stage 12 Blade Tip Clearance in a Simulated Typical Flight Mission.

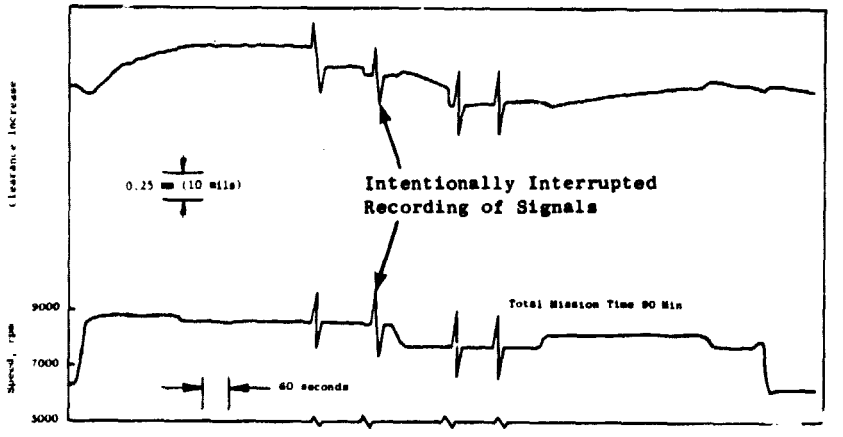

Figure 32. Small Variation of Stage 13 Blade Tip Clearance in a Simulated Typical Flight Mission.

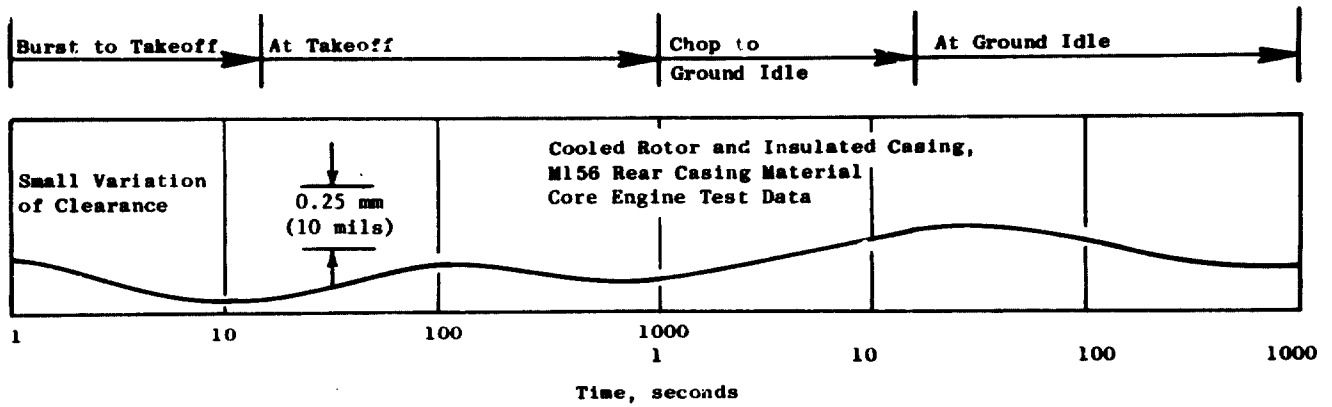

Figure 33. Proposed Improved Clearance Variations in Stage 13 After Burst and Chop Power-Throttle Movements.

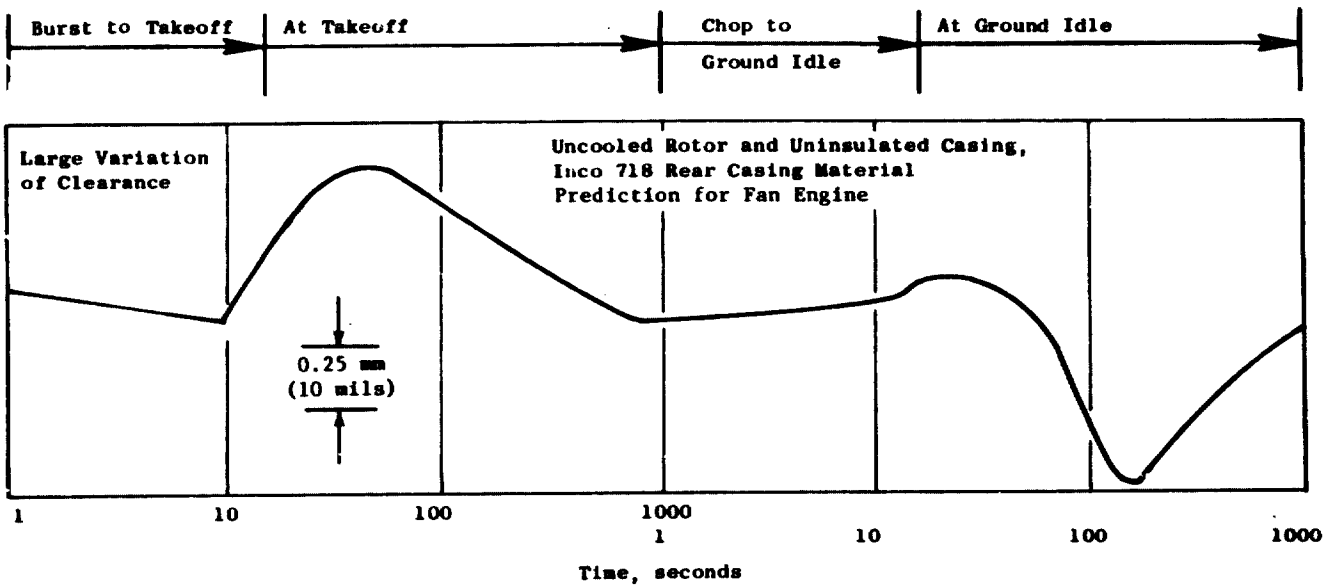

Figure 34. Current Clearance Variations in Stage 13 After Burst and Chop Power-Throttle Movements.

7.0 CONCLUSIONS

There were two objectives in this program. The first objective was to determine the effect of compressor airfoil tip clearance variations on compressor efficiency and hence on engine fuel consumption. The second objective was to investigate methods of potential improvements in compressor clearances.

In these investigations, instrumented core engine tests were conducted in which compressor rotor bore cooling was used for two different purposes. In the steady-state power calibrations it was used as a means of varying the compressor airfoil tip radial clearances from test-point-to-test-point. In this application it proved to be more effective than the pretest predictions indicated. Rotor bore temperature reductions of up to about 170°C (300°F) were produced, which in turn increased the clearances up to 0.63 mm (.025 in) in the aft stages of the compressor. The corresponding average normalized compressor clearance increase was calculated to be 0.6 percent, equivalent to a compressor efficiency increase of also 0.6 percent. For the same clearance change, the currently used derivative would indicate about 1.1 percent of compressor efficiency change.

The measured core engine fuel flow increase produced by the 0.6 percent average compressor clearance increase was 1.7 percent which is equivalent to about 0.3 percent in specific fuel consumption (SFC) of a CF6 fan engine at cruise. Using the current GE derivative, the 0.6 percent average clearance increase would increase SFC by 0.55 percent. The results of this program show that engine performance is much less sensitive to compressor clearance variation (about 50 percent) than the previous data and experience have indicated.

In the transient tests, which included power throttle bursts and chops and hot rotor power throttle rebursts, the compressor rotor bore cooling was maintained at a constant fraction of the engine air flow. It was used in these tests together with the stator casing insulation and the low coefficient of expansion of the stator casing material, as a means of improving compressor clearances in the aft stages of the compressor which have the greatest impact on the compressor performance.

The build-up and hence the steady-state compressor airfoil tip radial clearances depend on the clearance excursions during the engine transient operating conditions. The smaller the transient excursions the smaller the build-up and hence the steady-state operating clearances can be maintained. The transient clearance excursions in the instrumented core engine were much smaller than those predicted for the CF6-50 fan engine which does not have compressor rotor bore cooling, stator casing insulated structure and a low thermal coefficient of expansion of the rear stator casing material.

The calculations show that with the use of the above features the compressor clearances can be reduced by 1.0 mm (.040 in) in the aft stages (10 through 14). This would reduce the average normalized compressor clearance by 0.78 percent. Using the derivative obtained in this program the corresponding increase in compressor efficiency would also be 0.78 percent and the SFC of a fan engine would

be reduced by about 0.38 percent. Using the derivatives, currently in use at General Electric, these numbers would be 1.4 percent and 0.68 percent respectively. The reasons for the differences have not yet been determined. In either case the predicted improvements in performance are very significant.

APPENDIX A - SYMBOLS

HPC	High Pressure Compressor
SLS	Sea Level Static
ADH	Automatic Data Handling
IDR	Instrumentation Data Room
ECI	Engine Component Improvement
ACEE	Aircraft Energy Efficiency

APPENDIX B - REFERENCES

1. R.H. Wulf, "Engine Diagnostics Program, CF6-50 Engine Performance Deterioration, NASA CR-159867, November 1980.

APPENDIX C

QUALITY ASSURANCE

INTRODUCTION

The quality program applied to this contract is a documented system throughout the design, manufacture, repair, overhaul and modification cycle for gas turbine aircraft engines. The quality system has been constructed to comply with military specifications MIL-Q-9858A, MIL-I-45208, and MIL-STD-45662 and Federal Aviation Regulations FAR-145 and applicable portion of FAR-21.

The quality system and its implementation are defined by a complete set of procedures which has been coordinated with the DOD and FAA and has their concurrence. In addition, the quality system as described in the quality program meets the contractor requirements required by the NASA-Lewis Research Center. The following is a brief synopsis of the system.

QUALITY SYSTEM

The quality system is documented by operating procedures which coordinate the quality-related activities in the functional areas of Engineering, Manufacturing, Materials, Purchasing, and Engine Programs. The quality system is a single-standard system wherein all product lines are controlled by the common quality system. The actions and activities associated with determination of quality are recorded, and documentation is available for review.

Inherent in the system is the assurance of conformance to the quality requirements. This includes the performance of required inspections and tests. In addition, the system provides change control requirements which assure that design changes are incorporated into manufacturing, procurement and quality documentation, and into the products. Material used for parts is verified for conformance to applicable engineering specifications, utilizing appropriate physical and chemical testing procedures.

Measuring devices used for product acceptance and instrumentation used to control, record, monitor, or indicate results of readings during inspection and test are initially inspected and calibrated and periodically are reverified or recalibrated at a prescribed frequency. Such calibration is performed by technicians against standards which are traceable to the National Bureau of Standards. The gages are identified by a control number and are on a recall schedule for reverification and calibration. The calibration function maintains a record of the location of each gage and the date it requires recalibration. Instructions implement the provisions of MIL-STD-45662 and the appropriate FAR requirements.

Work sent to outside vendors is subject to quality plans which provide for control and appraisal to assure conformance to the technical requirements. Purchase orders issued to vendors contain a technical description of the work to be performed and instructions relative to quality requirements.

Engine parts are inspected to documented quality plans which define the characteristics to be inspected, the gages and tools to be used, the conditions under which the inspection is to be performed, the sampling plan, laboratory and special process testing, and the identification and record requirements.

Work instructions are issued for compliance by operators, inspectors, testers, and mechanics. Component part manufacture provides for laboratory overview of all special and critical processes, including qualification and certification of personnel, equipment and processes.

When work is performed in accordance with work instructions, the operator/inspector records that the work has been performed. This is accomplished by the operator/inspector stamping or signing the operation sequence sheet to signify that the operation has been performed.

Various designs of stamps are used to indicate the inspection of status of work in process and finished items. Performance or acceptance of special processes is indicated by distinctive stamps assigned specifically to personnel performing the process or inspection. Administration of the stamp system and the issuance of stamps are functions of the Quality Operation. The stamps are applied to the paperwork identifying or denoting the items requiring control. When stamping of hardware occurs, only laboratory approved ink is used to assure against damage.

The type and location of other part marking are specified by the design engineer on the drawing to assure effects do not compromise design requirements and part quality.

Control of part handling, storage and delivery is maintained through the entire cycle. Engines and assemblies are stored in special dollies and transportation carts. Finished assembled parts are stored so as to preclude damage and contamination, openings are covered, lines capped and protective covers applied as required.

Nonconforming hardware is controlled by a system of material review at the component source. Both a Quality representative and an Engineering representative provide the accept (use-as-is or repair) decisions. Nonconformances

are documented, including the disposition and corrective action if applicable to prevent recurrence.

The system provides for storage, retention for specified periods, and retrieval of nonconformance documentation. Documentation for components is filed in the area where the component is manufactured/inspected.

APPENDIX D

INSTRUMENTATION DESCRIPTION

The following test instrumentation was used to measured rotor cooling air inlet and exit conditions, engine performance, compressor blade tip clearances, temperatures and to monitor engine operation. The instrumentation is listed in three groups:

1. Special instrumentation used for this investigation
2. Engine performance instrumentation and
3. Engine control and safety instrumentation.

1. Special Instrumentation Used for this Investigation

- Compressor rotor cooling air temperature at inlet and exit - a total of four thermocouples.
- Compressor rotor cooling air pressure at inlet and exit - a total of four probes.
- Compressor Rotor Thermocouples - Fifty-four chromel/alumel thermocouples on the compressor rotor inner surfaces..
- Compressor Stator Thermocouples - A total of forty-eight skin thermocouples and three air thermocouples (all are chromel/alumel) were mounted on the outer surfaces of the stator casing.
- Casing Capacitance Clearanceometers - A total of nine clearanceometers were used.
- Casing Touch Probe Cleranceometers - A total of three, one in each plane of the capacitance clearanceometers were used.
- Calibrated Orifice Cooling Air Flow Measurement at inlet and exit.

2. Engine Performance Instrumentation

- Inlet Temperature - Chromel/alumel thermocouples attached to the bellmouth rakes.
- Core Inlet Temperature/Pressure - Ten flowpath wall static pressure taps and five rakes with five elements each for total pressure and temperature.
- Compressor Discharge Pressure - Four static pressure probes in the compressor rear frame.

- Compressor Discharge Total Pressure/Temperature - Five, 5-element rakes were used to measure compressor discharge total temperature and pressure.

- Turbine Mid Frame Discharge Temperature - Temperature in this plane was measured by a production-configuration EGT harness consisting of 11 dual-element thermocouple probes electrically averaged.

- Turbine Mid Frame Discharge Pressure - Pressure was measured using five probes, each having four elements feeding a single fitting.

3. Engine Control and Safety Instrumentation

- Barometric Pressure - The local barometric pressure measured using a recording Bendix Microbarograph.

- Humidity - The absolute humidity measured in grains of moisture per pound of dry air using a Foxboro humidity indicator.

- Cell Static Pressure - Test cell static pressure measured at four locations in the cell.

- Core Speed - Core rotor speed measured using a tach generator driven off the accessory gearbox.

- Main Fuel Flow - Fischer & Porter volumetric flowmeter, facility mounted.

- Verification Fuel Flow - Second fuel flowmeter mounted in series with WFMAIN.

- Fuel Temperature - Temperature of fuel measured at the facility flowmeters using a single copper/constantan probe in the fuel line.

- Fuel Sample Specific Gravity - Specific gravity of the fuel sample measured using a hydrometer.

- Fuel Sample Temperature - Fuel sample temperature measured during the specific gravity measurement.

- Variable Stator Vane Position - Readout of the LVDT attached to the high pressure compressor variable stator actuation lever.

Instrumentation accuracies are listed below. The quoted values are two standard devitation values with 95% confidence.

Parameter	
Core Speed	±10 rpm
Barometric Pressure	±0.007 psia
Relative Humidity	±5% reading
Fuel Specific Gravity	±0.15% reading
Fuel Sample Temperature	±0.5° F
Fuel Temperature	±2.5° F
Variable Vane Position	±2 degrees
Inlet Temperature	±1° F
Fuel Flow - Volumetric	±0.54% reading (20-100% power)
Cell Pressure	±0.05% full scale or ±0.4% reading whichever is greater
Compressor Discharge Pressure	±0.05% full scale or ±0.4% reading whichever is greater
Compressor Discharge Temperature	±6° F
TMF Discharge Temperature	±10° F
TMF Discharge Pressure	±0.05% full scale or ±0.4% reading whichever is greater
Dynamic Stress	±15%
Compressor Rotor & Stator Temperatures	±10° F
Core Inlet Temperature	±1° F
Core Inlet Pressure	±.05 full scale or ±0.4% reading whichever is greater
Clearanceometers (Capacitance)	±2 mils
Touch Probe	±2 mils
Compressor Rotor Cooling Flow	±1.0% of flow setting